Tribol Lett (2014) 53:199–206
DOI 10.1007/s11249-013-0257-0

ORIGINAL PAPER

Fatty Acid Adsorption on Several DLC Coatings Studied by Neutron Reflectometry

R. Simič · M. Kalin · T. Hirayama · P. Korelis · T. Geue

Received: 18 September 2013 / Accepted: 25 October 2013 / Published online: 7 November 2013

Abstract The application of diamond-like carbon (DLC) coatings on the contacts of mechanical systems is becoming widespread thanks to their excellent tribological properties. Numerous studies of DLC coatings have been reported over the past decade and, as a result, the understanding of their lubrication has improved. The tribological properties of boundary-lubricated contacts are drastically affected by adsorbed layers; however, due to the variety of lubricant additives and coating structures, no general adsorption mechanisms for DLC coatings have been put forward until now. This has, unfortunately, hindered improvements in their lubrication performance. Many of the essential physical properties of the adsorbed layers also remain undefined. In this work, we used neutron reflectometry to determine the thickness and the density of the adsorbed layers of fatty acid molecules on coatings of a-C, a-C:H, a-C:H:F and a-C:H:Si. The results showed that a 0.9-nm-thick layer adsorbed onto the a-C and a-C:H coatings. In contrast, both doped coatings, i.e. the a-C:H:F and a-C:H:Si, showed a poorer adsorption ability towards the fatty acid molecules than the a-C and a-C:H. Continuous adsorption layers were not detected on the a-C:H:F and a-C:H:Si; however, the possibility of adsorption in lower quantities cannot be ruled out.

Keywords DLC · Neutron reflectometry · Adsorption · Fatty acid

R. Simič · M. Kalin (✉)
Laboratory for Tribology and Interface Nanotechnology, Faculty of Mechanical Engineering, University of Ljubljana, Bogišićeva 8, 1000 Ljubljana, Slovenia
e-mail: mitjan.kalin@tint.fs.uni-lj.si

T. Hirayama
Department of Mechanical Engineering, Doshisha University, 1–3 Miyakodani, Tatara, Kyotanabe, Kyoto 610-0394, Japan

P. Korelis · T. Geue
Paul Scherrer Institut (PSI), 5232 Villigen, Switzerland

1 Introduction

The contacts of mechanical systems are subject to friction and wear, which result in energy loss, reduced functionality and increased maintenance costs. The application of diamond-like carbon (DLC) coatings, which are known for their very low-friction and exceptional anti-wear properties [1–3], can reduce energy losses and extend the lifetime of contacting surfaces. The low-friction properties of DLC coatings are assumed to originate partly from their chemical stability and general non-reactivity towards the surrounding molecules [4]. However, limited interactions with surrounding molecules hinder the possibility of improving the lubrication performance of DLC. Nevertheless, it has been shown that DLC coatings can interact with the surrounding environmental or lubricant molecules, especially under tribocontact conditions, which generally enhance the chemical reactions. The tribochemical reactions of DLC were observed in several cases, from interactions with simple gaseous species [4–7] and water molecules [8, 9] to more complex additives, like ZDDP and MoDTC [10–12]. Generally accepted mechanisms for the interactions with basic molecules and their functional parts such as hydroxyl and carboxyl groups, which are present in oils and additives and are known to improve the tribological properties of steel [13–16], have not yet been established. Determining the nature of these mechanisms represents an experimental challenge, which is only increased by the

variety of the tribological effects that occur in the contacts and the complexity of the structure of most additives. A thorough understanding of the lubrication mechanisms of DLC coatings can be the foundation for engineering improvements in lubrication efficiency, by adapting the formulated lubricants and coatings to achieve an optimum lubrication performance.

Hydrogen is known to affect the friction of DLC coatings by reacting with the surface dangling bonds and creating a passive H-terminated surface layer, which prevents strong adhesion bonds from forming between the contacting surfaces, and therefore enables low friction [4–7]. It was also shown that water molecules can tribochemically react with DLC, whereby the hydroxyl groups form on the surface, causing OH termination, which provides protection from the adhesion bonds [8, 9]. OH termination was also observed on ta-C surfaces when either glycerol or glycerol-mono-oleate (GMO) molecules were present in the lubricant under boundary lubrication conditions [17, 18]. The hydroxyl groups from the glycerol and the GMO were assumed to interact with the friction-activated ta-C surfaces causing OH termination. It has been suggested that surface hydroxylation enables the intercalation of the surrounding alcohol molecules, which adsorb onto the surface OH groups via hydrogen bonding and thus help decrease the friction. An enhancing effect of alcohols on the tribological properties of DLC coatings was also reported in other studies [17–19], and some adsorption mechanisms for alcohols and hydroxyl-containing molecules have been proposed [18–21]. In addition, we have shown in our previous studies that an indisputable correlation exists between the tribological performance and the adsorption ability of the coatings [19, 22]. Adsorption ability also seems to be related to the surface polarity, which was suggested to play an important role in tailoring the wetting properties and the related tribochemical interactions of DLC coatings [23]. Due to the specificity of the compounds and the challenges in experimental investigations, the application of the suggested adsorption mechanisms is not universal. In addition, little is known about the strength of the adsorption, the conditions under which adsorption occurs, which polar molecules are better at adsorbing, or about the physical properties of the adsorbed layers, such as the thickness and the density, which crucially affect the tribological properties of DLC coatings.

A suitable technique with sub-nanoscale precision for examining such solid–liquid interfaces is neutron reflectometry (NR), which is used for the detection and examination of adsorbed layers on metal surfaces [24]. Neutrons do not interact with electrons but with atomic nuclei and are therefore able to penetrate deep into the material without affecting its chemistry and physical properties. Neutrons are scattered by light atoms such as hydrogen and carbon, which makes them convenient for the analysis of the interfaces between the hydrocarbon lubricants and the hard carbon coatings. Since deuterium can be distinguished from hydrogen, the deuterium substitution of hydrogen in molecules can be used for labelling and distinguishing these molecules from the non-deuterated ones. Neutrons scattered in the layered materials provide information about the physical properties of the layers, like the thickness and the density.

We used NR to determine the thickness and the density of the adsorbed layers on DLC coatings. The adsorption of alcohols on various DLC surfaces was investigated in a previous study [25]; however, in this work, we examined the fatty acid adsorption on various DLC coatings, because fatty acids are proven to improve the boundary lubrication of steel and DLC [22] and were shown to be even more effective than alcohols [13, 26]. We focused on the adsorption of fatty acids on a-C, a-C:H, a-C:H:F and a-C:H:Si coatings. The a-C and a-C:H were selected to examine the effect of hydrogen on the adsorption ability of the coatings. Doping of the a-C:H was chosen to alter the reactivity of the coating, making it either less reactive in case of F-doped DLC [27] or more reactive in case of Si-doped and oxidized DLC coating [23, 28, 29]. The results of the current study give direct evidence for how the various coating structures and types of doping elements affect the carboxylic group adsorption and provide some insight into the DLC boundary lubrication mechanisms, which supports the improvements in the tribological performance of DLC coatings.

2 Experimental

2.1 Samples

The substrates for the coating deposition were ultra-flat silicon blocks, $50 \times 50 \times 10$ mm^3 in size, with one side polished to a surface roughness of $R_q = 0.3$ nm (Yamanaka Semiconductor Co., Japan). Four types of DLC coatings (a-C, a-C:H, a-C:H:F, a-C:H:Si) were deposited on the polished side of the blocks. The a-C coating was deposited using DC magnetron sputtering with Ar as a sputtering gas at a pressure of 1.3 Pa. The a-C:H coating was deposited using a 13.56-MHz radio frequency plasma-assisted CVD (RF PACVD) process and was a typical non-doped, hydrogenated, amorphous DLC coating with a H-content of 32 at.% and a $sp^3/(sp^3 + sp^2)$ ratio of 35–40 %. The F-doped coating was deposited in a similar way as the a-C:H, with fluorine being added in the gas phase. The obtained coating contained 6.5 at.% of F at the surface. The Si-doped DLC was a variant of the F-doped DLC coating, with Si being used instead of F in the gas

Table 1 Composition, thickness and surface roughness R_q of the coatings

Coating	C (at.%)	H (at.%)	F (at.%)	Si (at.%)	Thickness (nm)	R_q (AFM) (nm)
a-C	>99	/	/	/	≈40	1.5
a-C:H	68	32	/	/	≈53	2.1
a-C:H:F	72	21	6.5	/	≈53	2.1
a-C:H:Si	58.5	37	/	2.5	≈53	1.5

Table 2 Properties of the base oil and the additive

	PAO6	d-Hexadecanoic acid
Chemical formula	$C_{10}H_{21}$–$(C_{10}H_{20})_n$–H	$C_{15}D_{31}COOH$
Density ρ (at 25 °C) (g/cm^3)	0.828	0.954
Scattering length density *Nb* (Å^{-2})	-0.37×10^{-6}	6.41×10^{-6}

phase. The a-C:H:Si coating contained 2.5 at.% of Si at the surface. The elemental composition, the thickness and the final surface roughness measured with the AFM of the coatings are listed in Table 1. The samples were not exposed to any solvent (e.g. for cleaning) prior to the experiment, to avoid any contamination and passivation of the surfaces with the cleaning solvents. Any dust particles that may have been present on the surface were removed by a stream of dry air.

2.2 Liquids

High-purity, deuterated, hexadecanoic acid (98 at.% D, Sigma-Aldrich Co., LLC.) was used as a surface-active agent to study the reaction of the DLC coatings with the carboxyl end-groups that are commonly present in various additives. The hexadecanoic acid was dissolved in PAO6 oil (Neste Oil, Espoo, Finland) in a concentration of 20 mmol/l, which corresponds to a mass concentration of 0.69 wt%. Deuterium-substituted fatty acid molecules were used to distinguish the adsorbed additive layer from the rest of the solution. Bulk deuterated hexadecanoic acid has a very different *scattering length density* (*SLD)* for neutrons than non-deuterated hydrocarbon like PAO oil (see Table 2). The SLD is the product of the atomic density *N* times the characteristic scattering length for each element *b* and is therefore usually denoted by the product *Nb*.

2.3 Neutron Reflectometer

The neutron reflectometer was the Apparatus for Multi-Option Reflectometry (AMOR), which is located at the continuous spallation neutron source (SINQ) at the Paul Scherrer Institute (PSI) in Switzerland. The AMOR is an energy-dispersive reflectometer that operates in a neutron wavelength range of 3.5 Å $< \lambda <$ 12 Å with a time-of-fight (TOF) detection mode. At the instrument position, the continuous neutron beam is pulsed using two choppers. A set of three slits was used to obtain the beam footprint of approximately 40 × 40 mm^2 on the sample's surface. Two slits were used to select only the specular reflection of the reflected neutron beam at an angle 2θ with respect to the incident beam. The sample reflectivity was calculated as the ratio of the reflected to incident beam intensities. Reflectivity in the graphs is presented as a function of the momentum transfer vector $\vec{q}$, the length of which is equal to $q_z = (4\pi/\lambda)\ \sin\theta$. A schematic image of the specular reflection and the momentum transfer vector $\vec{q}$ is presented in Fig. 1. Since AMOR is an energy-dispersive reflectometer, measurements at two incident angles (i.e. $\theta = 0.5°$ and 1.3°) were needed to obtain the reflectivity in the range 0.01 Å$^{-1} < q_z <$ 0.07 Å^{-1}.

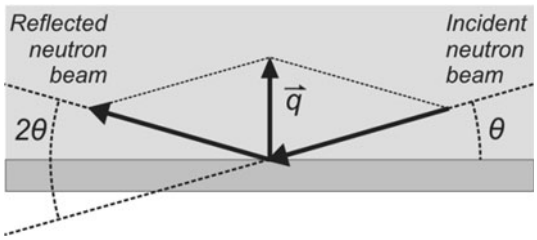

Fig. 1 Specular reflection of a neutron beam

2.4 Procedure

To obtain the thickness and the density of the adsorbed layers, the following experimental procedure was performed, as shown in Fig. 2. First, each sample was mounted on a sample holder, and pure PAO oil was introduced into the holder. Special care was taken to displace all the air bubbles. A reflectivity profile was obtained for the DLC–PAO interface in order to reveal the coating thickness and the vertical distribution of the SLD. In the second step, the pure PAO oil was exchanged for the hexadecanoic acid and the PAO solution. The measurement was taken approximately 6 h after the time the exchange was made, to allow the fatty acid to adsorb onto the DLC. In the event that an adsorption layer was formed, the reflectivity profile was expected to shift with respect to the reflectivity profile from the first step. After obtaining the results, the reflectivity profiles were analysed and fitted using a theoretical model based on the Parratt formalism [30]. The measurement resolution was $\Delta q_z/q_z = 0.03$, and this was taken into account during the data fitting.

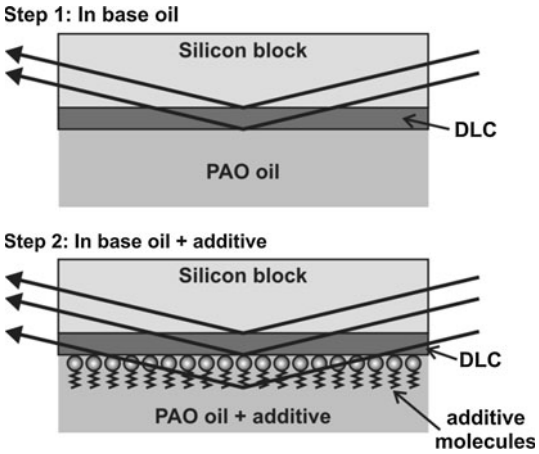

Fig. 2 Experimental procedure for studying the adsorption layers using neutron reflectometry. The reflectivity from the sample surface in the PAO was measured first. Then, after exchanging the PAO for a solution of PAO and the additive, the reflectivity was obtained again to check for changes due to the formation of adsorbed layers

The results of the analysis are given in the graphs as the reflectivity profiles for each coating. The horizontal axis of the graphs corresponds to the length of the momentum transfer vector q_z. The reflectivity on the vertical axis corresponds to the reflected beam intensity, normalized to the incident beam intensity and scaled to 1. The reflectivity profiles presented in the graphs for the second step are offset by one order of magnitude along the *y*-axis to make it easier to distinguish the individual reflectivity profiles. The optimum fitting curves based on the Parratt formalism are also presented for each measurement. To obtain the optimum fit, the interfacial roughness had to be considered. This was done by assuming that the SLD gradient at a given interface follows a Gaussian distribution with standard deviation σ. It should be noted that the surface roughness, the uneven layer thickness and the interface gradient affect the reflectivity in a similar way and therefore cannot be distinguished individually in the scattering data.

3 Results

3.1 a-C Coating

Figure 3a presents the reflectivity profiles for the a-C coating. Fitting the data obtained in pure PAO revealed the thickness of the coating to be 40.8 nm, Fig. 3b. The SLD, which was assumed to be constant over the thickness of the coating, was calculated to be 5.1×10^{-6} Å^{-2}. The interfacial roughness was estimated to be $\sigma = 1.5$ nm at the coating/substrate interface and $\sigma = 1.4$ nm at the coating surface. When the a-C surface was exposed to the hexadecanoic acid solution, the reflectivity profile shifted

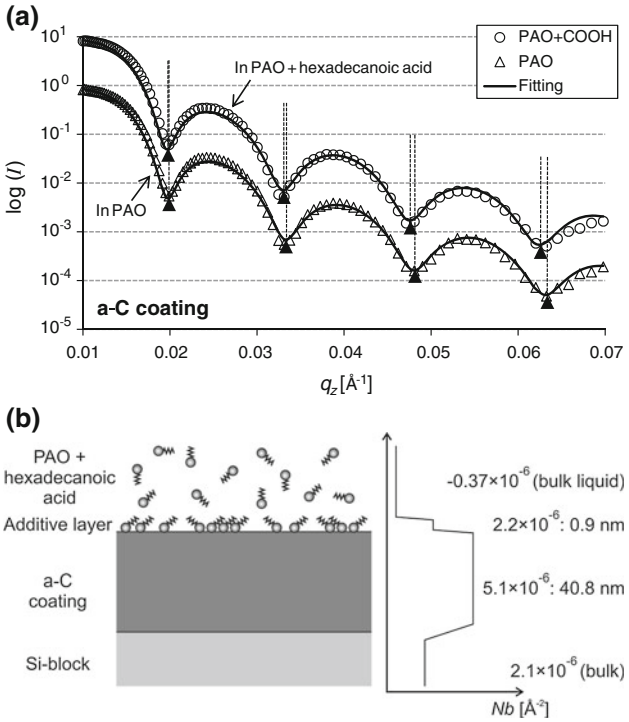

Fig. 3 **a** Neutron reflectometry profiles for the a-C coating. Data obtained in PAO + COOH is scaled by one order of magnitude for clarity. *Black lines* represent fitting of the data, and *black triangles mark* the local minima of the fitting *curve*. **b** Schematic layer structure and *Nb* profile for the a-C coating in PAO + hexadecanoic acid, extracted from fitting the NR data

towards lower q_z values, resulting in narrower fringes, Fig. 3a. The fitting of the data revealed that a 0.9-nm-thick layer with a SLD of 2.2×10^{-6} Å^{-2} had formed on the surface, Fig. 3b. Since the SLD value of the bulk d-hexadecanoic acid is around 6.4×10^{-6} Å^{-2}, the density of the layer was calculated to be about 35 % of the density of the bulk hexadecanoic acid. The thickness of the detected layer was lower than the length of the hexadecanoic acid molecule, which is around 2.5 nm. The adsorbed molecules were thus assumed to be arranged at an angle to the surface, as suggested in Fig. 3b.

3.2 a-C:H Coating

The reflectivity profiles obtained for the a-C:H coating are presented in Fig. 4a. Fitting of the data obtained in the PAO revealed a 54.2-nm-thick coating, where the SLD was estimated to be 4.3×10^{-6} Å^{-2} and constant over the whole thickness of the coating, Fig. 4b. The SLD of the a-C:H was lower compared to the a-C, which is mainly due to the increased incoherent scattering from the coating because of the hydrogen content. The fitting revealed a roughness of $\sigma = 4.4$ nm at the substrate/coating interface and $\sigma = 1.6$ nm at the coating surface. The slightly larger interface roughness compared to the a-C coating caused the

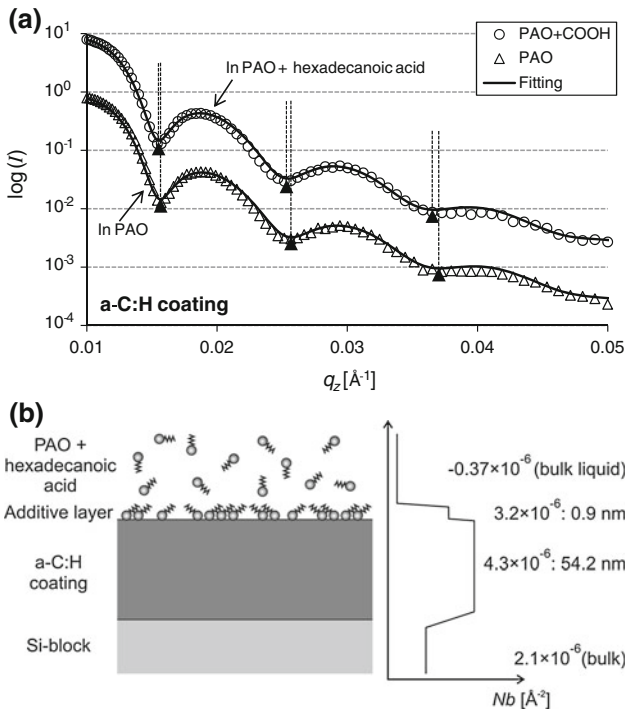

Fig. 4 **a** Neutron reflectometry profiles for the a-C:H coating. Data obtained in PAO + COOH are scaled by one order of magnitude for clarity. *Black lines* represent fitting of the data, and *black triangles mark* the local minima of the fitting *curve*. **b** Schematic layer structure and *Nb* profile for the a-C:H coating in PAO + hexadecanoic acid, extracted from fitting the NR data

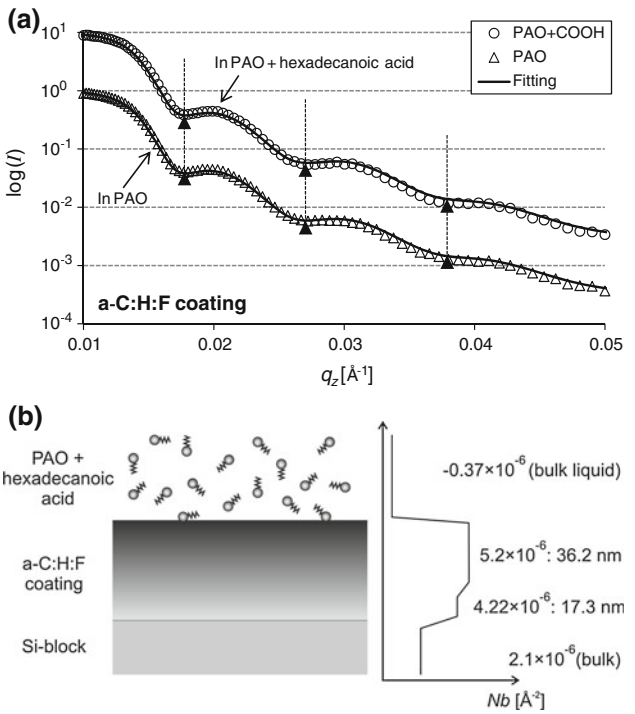

Fig. 5 **a** Neutron reflectometry profiles for the a-C:H:F coating. Data obtained in PAO + COOH are scaled by one order of magnitude for clarity. *Black lines* represent fitting of the data, and *black triangles mark* the local minima of the fitting *curve*. **b** Schematic layer structure and *Nb* profile for the a-C:H:F coating in PAO + hexadecanoic acid, extracted from fitting the NR data

intensity of the reflectivity fringes to attenuate faster towards increasing q_z values. When the PAO was exchanged for the PAO + hexadecanoic acid solution, the fringes became narrower, shifting the reflectivity profile towards lower q_z values, Fig. 4a. The fitting of the data showed that hexadecanoic acid formed a 0.9-nm-thick adsorbed layer on the a-C:H surface, Fig. 4b. The SLD of the layer was estimated to be 3.2×10^{-6} Å^{-2}, indicating that the density of the layer was approximately 50 % of the bulk density.

3.3 a-C:H:F Coating

The reflectivity profiles obtained for the a-C:H:F coating are presented in Fig. 5a. The fitting revealed a 53.5-nm-thick coating. This coating appeared to consist of two layers that were joined by a gradient transition, Fig. 5b. The first layer on the substrate was 17.3 nm thick with a SLD of 4.22×10^{-6} Å^{-2}. The second, topmost layer was 36.2 nm thick with a SLD of 5.2×10^{-6} Å^{-2}. The gradient between the two layers was estimated to have a σ of about 9.0 nm. The SLD of the first layer therefore resembles the SLD of the a-C:H. The somewhat faster attenuation of the reflectivity fringes towards higher q_z values may again be due to the relatively greater roughness of $\sigma = 5.0$ nm at the substrate/coating interface and $\sigma = 1.6$ nm at the coating surface. Exchanging the PAO for the PAO + hexadecanoic acid solution resulted in no changes to the reflectivity profile, Fig. 5a. This suggests that hexadecanoic acid molecules did not form a continuous adsorbed layer on the surface of the a-C:H:F, as presented in Fig. 5b.

3.4 a-C:H:Si Coating

The reflectivity profiles obtained for the a-C:H:Si coating are presented in Fig. 6a. The a-C:H:Si coating exhibited a gradient structure and a relatively thick diffusion zone at the substrate/coating interface, Fig. 6b. The fitting revealed that the coating is composed of two layers joined by a gradient transition, similar to the a-C:H:F. The first layer of the coating was around 5.0 nm thick with a SLD of 4.1×10^{-6} Å^{-2}, which is close to pure a-C:H. The second, topmost, layer was 47.8 nm thick with a SLD of 3.4×10^{-6} Å^{-2}. The gradient between the two layers had $\sigma = 2.1$ nm. Therefore, the total thickness of both layers was 52.8 nm, which is similar to the a-C:H and the a-C:H:F. The roughness on the surface of the coating was estimated to be $\sigma = 1.1$ nm. A diffusion zone with a thickness of 27 nm was considered at the substrate/coating interface, which occurred due to the nature of the bonding

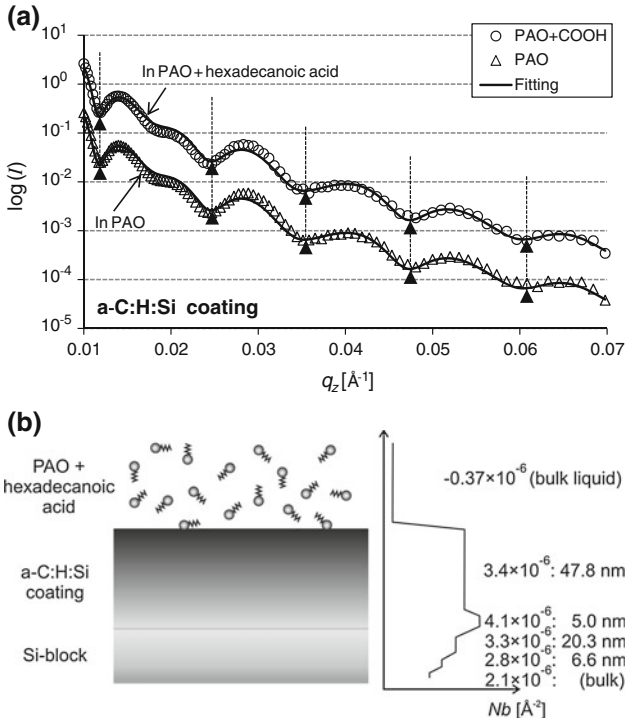

Fig. 6 **a** Neutron reflectometry profiles for the a-C:H:Si coating. Data obtained in PAO + COOH are scaled by one order of magnitude for clarity. *Black lines* represent fitting of the data, and *black triangles mark* the local minima of the fitting *curve*. **b** Schematic layer structure and *Nb* profile for the a-C:H:Si coating in PAO + hexadecanoic acid, extracted from fitting the NR data

between the silicon substrate and the a-C:H:Si coating. The optimum fit was achieved by splitting the diffusion zone into two layers to obtain a gradual decrease in the SLD from the coating to the bulk substrate, Fig. 6b. The diffusion layer closest to the substrate/coating interface had a SLD of 3.2 $\times$ 10^{-6} Å^{-2} and a thickness of 20.3 nm, while the bottom interlayer had a SLD of 2.8 $\times$ 10^{-6} Å^{-2} and a thickness of 6.6 nm. The SLD value of the silicon block was 2.1 $\times$ 10^{-6} Å^{-2}. The gradients between these layers were in the range 2.8–4.0 nm to smooth out the layered model, Fig. 6b. When the PAO was exchanged for the hexadecanoic acid solution, the reflectivity profile remained generally unchanged. Only a slight shift towards lower q_z values was observed with some of the data points; however, the fitting of the reflectivity profile revealed no adsorbed layers on the a-C:H:Si surface, Fig 6b.

4 Discussion

4.1 a-C Coating

The results show that the hexadecanoic acid molecules adsorbed onto the surface of the a-C coating in static conditions form a relatively thin, 0.9-nm adsorbed layer. The density of the layer was estimated to be roughly one-third of the density of the bulk hexadecanoic acid. Since neutron reflectometry does not provide information about the chemical structure of the adsorbed film, we cannot state, based on these results, whether this layer was chemisorbed or physisorbed. Nevertheless, this coating proved to promote adsorption. One of the reasons for this high reactivity could be the lack of hydrogen during the deposition process, meaning that the surface dangling bonds could not be passivated by the hydrogen that would otherwise make the coating less reactive. If the surface dangling bonds were not passivated by environmental species during the time of the experiment, the hexadecanoic acid most probably could be chemisorbed to the dangling bonds of the surface carbon atoms. On the other hand, surface dangling bonds might also become passivated by the time of the experiment due to the exposure to environmental molecules. In this case, the hexadecanoic acid could most probably be physisorbed by hydrogen bonding to the surface oxides and hydroxides.

4.2 a-C:H Coating

The results show that an adsorption layer of the same thickness as on the a-C also formed on the a-C:H. Although the detected adsorbed layer on the a-C:H was slightly more dense than the layer on the a-C, it seems that the a-C and a-C:H both have a relatively similar and rather good adsorption ability towards fatty acid molecules. Although hydrogenation usually decreases the reactivity of the coating, the results of this study suggest that the incorporation of hydrogen into the coating did not substantially affect the coating's adsorption ability towards hexadecanoic acid. This differs from the results of our previous study on similar coatings, where hydrogenation decreased the adsorption ability towards hexadecanol molecules [25]. In that study hexadecanol formed adsorbed layers only on the a-C and not on the a-C:H. This difference between fatty acids and alcohols can be explained by the higher polarity of the fatty acids compared to the corresponding alcohols, which results in a better adsorption ability of the fatty acids compared to the alcohols. This has already been shown with a-C:H coatings, where fatty acids proved to be better at adsorbing than the corresponding alcohols [26]. The results of the current study therefore suggest that the polarity of the fatty acids was sufficient to cause relatively similar adsorption onto the non-hydrogenated a-C coating and the hydrogen-containing a-C:H.

4.3 a-C:H:F Coating

The results show no adsorption layers of hexadecanol on the surface of the a-C:H:F coating. This result does not

suggest the complete absence of adsorption on the a-C:H:F, but rather that a continuous layer was not formed. We have to note that the NR profile was obtained by neutron scattering from a surface area of approximately 40 × 40 mm^2, and the result actually represents an average reflectivity profile for the whole illuminated sample volume. In the case that adsorption appeared on a small fraction of the sample's surface, the reflectivity profile might remain unaltered. This means that adsorption in small quantities is a possibility. Therefore, the incorporation of fluorine into the DLC coating did not increase, but rather decreased the adsorption ability of the coating. This result is in agreement with the results of a recent study [23] where the polar component of the surface energy for a-C:H:F was much lower compared to all the other, doped and non-doped, DLC coatings. This indicates the extremely low reactivity of the a-C:H:F towards the adsorption of polar molecules. It has also been shown in the case of glycine, which contains a carboxylic group at one end, that low F-doping may increase the adsorption of glycine, while increased doping levels lead to reduced adsorption compared to non-doped DLC [31]. Our results therefore agree with previous observations and strengthen the finding that fluorine doping decreases the ability of DLC towards the adsorption of carboxylic end-groups.

4.4 a-C:H:Si Coating

A detailed look at the measured raw NR data revealed a minor shift of some data points in the reflectivity profile of the a-C:H:Si coating when hexadecanoic acid was introduced. However, these changes were small, so that by fitting the NR data, the formation of an adsorbed layer on the a-C:H:Si could not be resolved. Doping of the DLC with Si therefore appeared to decrease the adsorption ability towards hexadecanoic acid compared to the non-doped a-C:H. However, this is contrary to what the surface energies of the coatings suggest. The a-C:H:Si possesses a higher polar component of surface energy, and therefore, a higher susceptibility towards polar molecule adsorption compared to the a-C:H [23]. Moreover, the a-C:H:Si proved to allow better adsorption of molecules with hydroxyl end-groups compared to the pure a-C:H [25, 32]. Therefore, by considering the small changes in the reflectivity in the present case and for previously reported results, it is reasonable to assume that some fatty acid molecules may still adsorb onto the a-C:H:Si, but their quantity was too low to form a continuous layer and be detected with the NR. Moreover, it was also shown in a recent study that the concentration of Si-dopant affects the adsorption ability of glycine (highly polar with a carboxylic end-group) on Si-doped DLC coatings and can, with increasing Si-concentrations, also decrease the glycine adsorption [33]. Therefore, the adsorption of fatty acid to Si-based DLC is proven to be highly feasible, but very sensitive to various factors, among which is the level of doping. Accordingly, in this study, in spite of the expected improved adsorption of fatty acid onto the a-C:H:Si coating, an inappropriate or non-optimized Si-concentration can be the reason for its lower adsorption compared to the non-doped a-C:H coating.

5 Conclusions

1. A relatively dense and thin adsorbed film of hexadecanoic acid formed on the surface of the non-hydrogenated a-C coating.
2. An adsorption layer of similar thickness as on the a-C also formed on the a-C:H.
3. The incorporation of F into the a-C:H coating decreased the ability of the DLC with respect to fatty acid adsorption, which agrees well with the low polar component of the surface energy of the a-C:H:F, and previous results.
4. The incorporation of Si decreased the ability of the DLC coating to adsorb fatty acid molecules, which contrasts with its higher polar component of surface energy compared to the non-doped a-C:H and also to our previous results with alcohol adsorption. The reason for the lower adsorption ability of the a-C:H:Si towards fatty acid compared to the non-doped a-C:H coating in this study may be attributed to the inappropriate or non-optimized Si-concentration in the DLC.
5. The absence of continuous adsorbed layers on the a-C:H:F and a-C:H:Si does not exclude adsorption, since the quantity and arrangement of the adsorbed molecules could be below the detection ability of the NR. Both doped coatings (a-C:H:F and a-C:H:Si) showed a poorer adsorption ability with respect to fatty acid molecules compared to the non-doped a-C and a-C:H.

Acknowledgments The authors greatly appreciate the generous support of the Taiho Kogyo Tribology Research Foundation, Japan, and also express their gratitude to Dr. T. Takeno, Prof. K. Adachi and Prof. T. Takagi (Tohoku University, Sendai, Japan) for their help with preparing the a-C coating, as well as to F. Meunier (Sulzer Sorevi, Limoges, France) for providing the a-C:H, a-C:H:F and a-C:H:Si coatings.

References

1. Robertson, J.: Diamond-like amorphous carbon. Mater. Sci. Eng. R. **37**, 129–281 (2002)
2. Erdemir, A.: Diamond-like carbon films, pp. 139–156. ASME Press, New York (2004)

3. Neville, A., Morina, A., Haque, T., Voong, M.: Compatibility between tribological surfaces and lubricant additives—how friction and wear reduction can be controlled by surface/lube synergies. Tribol. Int. **40**, 1680–1695 (2007)
4. Erdemir, A., Donnet, C.: Tribology of diamond-like carbon films: recent progress and future prospects. J. Phys. D Appl. Phys. **39**, R311–R327 (2006)
5. Fontaine, J., Donnet, C., Grill, A., LeMogne, T.: Tribochemistry between hydrogen and diamond-like carbon films. Surf. Coat. Technol. **146–147**, 286–291 (2001)
6. Erdemir, A.: The role of hydrogen in tribological properties of diamond-like carbon films. Surf. Coat. Technol. **146–147**, 292–297 (2001)
7. Li, H., Xu, T., Wang, C., Chen, J., Zhou, H., Liu, H.: Tribochemical effects on the friction and wear behaviors of a-C:H and a-C films in different environment. Tribol. Int. **40**, 132–138 (2007)
8. Wu, X., Ohana, T., Tanaka, A., Kubo, T., Nanao, H., Minami, I., Mori, S.: Tribochemical investigation of DLC coating in water using stable isotopic tracers. Appl. Surf. Sci. **254**, 3397–3402 (2008)
9. Guo, H., Qi, Y.: Environmental conditions to achieve low adhesion and low friction on diamond surfaces. Model. Simul. Mater. Sci. Eng. **18**, 034008 (2010)
10. de Barros Bouchet, M.I., Martin, J.M., Le-Mogne, T., Vacher, B.: Boundary lubrication mechanisms of carbon coatings by MoDTC and ZDDP additives. Tribol. Int. **38**, 257–264 (2005)
11. Equey, S., Roos, S., Mueller, S., Hauert, R., Spencer, N.D., Crockett, R.: Tribofilm formation from ZnDTP on diamond-like carbon. Wear **264**, 316–321 (2008)
12. Topolovec-Miklozic, K., Lockwood, F., Spikes, H.: Behaviour of boundary lubricating additives on DLC coatings. Wear **256**, 1893–1901 (2008)
13. Hardy, W., Doubleday, I.: Boundary lubrication. The paraffin series. Proc. R. Soc. A **100**, 550–574 (1922)
14. Bowden, F.P., Gregory, J.N., Tabor, D.: Lubrication of metal surfaces by fatty acids. Nature **156**, 97–101 (1945)
15. Hu, Y., Liu, W.: Tribological properties of alcohols as lubricating additives for aluminum-on-steel contact. Wear **218**, 244–249 (1998)
16. Przedlacki, M., Kajdas, C.: Tribochemistry of fluorinated fluids hydroxyl groups on steel and aluminum surfaces. Tribol. Trans. **49**, 202–214 (2006)
17. Kano, M., Yasuda, Y., Okamoto, Y., Mabuchi, Y., Hamada, T., Ueno, T., Ye, J., Konishi, S., Takeshima, S., Martin, J.M., de Barros Bouchet, M.I., Le Mogne, T.: Ultralow friction of DLC in presence of glycerol mono-oleate (GMO). Tribol. Lett. **18**, 245–251 (2005)
18. Matta, C., Joly-Pottuz, L., de Barros Bouchet, M.I., Martin, J.M., Kano, M., Zhang, Q., Goddard III, W.A.: Superlubricity and tribochemistry of polyhydric alcohols. Phys. Rev. B **78**, 085436 (2008)
19. Kalin, M., Simič, R.: Atomic force microscopy and tribology study of the adsorption of alcohols on diamond-like carbon coatings and steel. Appl. Surf. Sci. **271**, 317–328 (2013)
20. Kasai, P.H., Shimizu, T.: Bonding of hard disk lubricants with OH-bearing end groups. Tribol. Lett. **46**, 43–47 (2012)
21. Shukla, N., Gellman, A.J., Gui, J.: The interaction of CF_3CH_2OH and $(CF_3CF_2)_2O$ with amorphous carbon films. Langmuir **16**, 6562–6568 (2000)
22. Simič, R., Kalin, M.: Adsorption mechanisms for fatty acids on DLC and steel studied by AFM and tribological experiments. Appl. Surf. Sci. **283**, 460–470 (2013)
23. Kalin, M., Polajnar, M.: The correlation between the surface energy, the contact angle and the spreading parameter, and their relevance for the wetting behaviour of DLC with lubricating oils. Tribol. Int. **66**, 225–233 (2013)
24. Hirayama, T., Torii, T., Konishi, Y., Maeda, M., Matsuoka, T., Inoue, K., Hino, M., Yamazaki, D., Takeda, M.: Thickness and density of adsorbed additive layer on metal surface in lubricant by neutron reflectometry. Tribol. Int. **54**, 100–105 (2012)
25. Kalin, M., Simič, R., Hirayama, T., Geue, T., Korelis, P.: Neutron-reflectometry of alcohol adsorption on various DLC coatings. Appl. Surf. Sci. (2013). doi:10.1016/j.apsusc.2013.10.047
26. Simič, R., Kalin, M.: Comparison of alcohol and fatty acid adsorption on hydrogenated DLC coatings studied by AFM and tribological tests. J. Mech. Eng. (2013, in press)
27. Donnet, C.: Recent progress on the tribology of doped diamond-like and carbon alloy coatings: a review. Surf. Coat. Technol. **100**, 180–186 (1998)
28. Grischke, M., Hieke, A., Morgenweck, F., Dimigen, H.: Variation of the wettability of DLC-coatings by network modification using silicon and oxygen. Diam. Relat. Mater. **7**, 454–458 (1998)
29. Roy, R.K., Choi, H.-W., Park, S.-J., Lee, K.-R.: Surface energy of the plasma treated Si incorporated diamond-like carbon films. Diam. Relat. Mater. **16**, 1732–1738 (2007)
30. Parratt, L.G.: Surface studies of solids by total reflection of X-rays. Phys. Rev. **95**, 359–370 (1954)
31. Ahmed, M.H., Byrne, J.A., McLaughlin, J.: Evaluation of glycine adsorption on diamond like carbon (DLC) and fluorinated DLC deposited by plasma-enhanced chemical vapour deposition (PECVD). Surf. Coat. Technol. **209**, 8–14 (2012)
32. Choi, J., Kawaguchi, M., Kato, T., Ikeyama, M.: Deposition of Si-DLC film and its microstructural, tribological and corrosion properties. Microsyst. Technol. **13**, 1353–1358 (2007)
33. Ahmed, M.H., Byrne, J.A., McLaughlin, J., Elhissi, A., Ahmed, W.: Comparison between FTIR and XPS characterization of amino acid glycine adsorption onto diamond-like carbon (DLC) and silicon doped DLC. Appl. Surf. Sci. **273**, 507–514 (2013)